UNIST NThRS

(Nuclear Thermal-hydraulics and Reactor Safety)

Effect of Filling Ratio on the Entrainment Limit of Large-Scale Heat Pipe with 3D-Printed Wick Structure

2024.10.24

Faruk Celik, Dong Hun Lee, Ye Yeong Park, In Cheol Bang*

Department of Nuclear Engineering, Ulsan National Institute of Science and Technology (UNIST)

ULSAN NATIONAL INSTITUTE OF SCIENCE AND TECHNOLOGY

Table of Contents

I. Introduction

➢ Heat Pipe Cooled Microreactors

- Microreactors, a subset of Small Modular Reactors (SMRs), are designed to produce electricity in the range of 1–20 MWe.
- The micro reactors have been developed for space applications, military bases and transportable solutions (by Westinghouse, LANL, INL, MIT, Oklo power etc.).
- Typically cooled by liquid metal heat pipes (HPs).
- The primary heat exchanger condense the vapor in the condenser region of HPs.
- These systems use heat pipes to transfer heat from the reactor core to power conversion mechanisms efficiently and passively.

Fig 1. eVinci micro reactor overview.

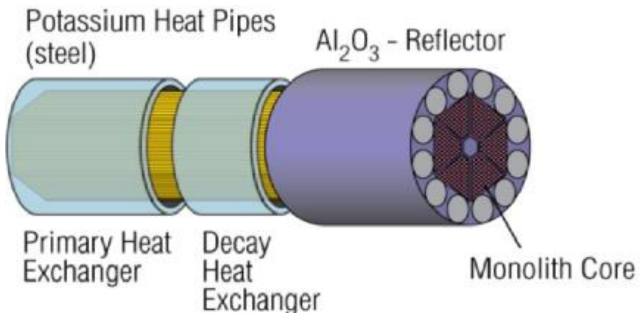

Fig 2. Special purpose reactor.

Fig 3. Aurora micro reactor overview.

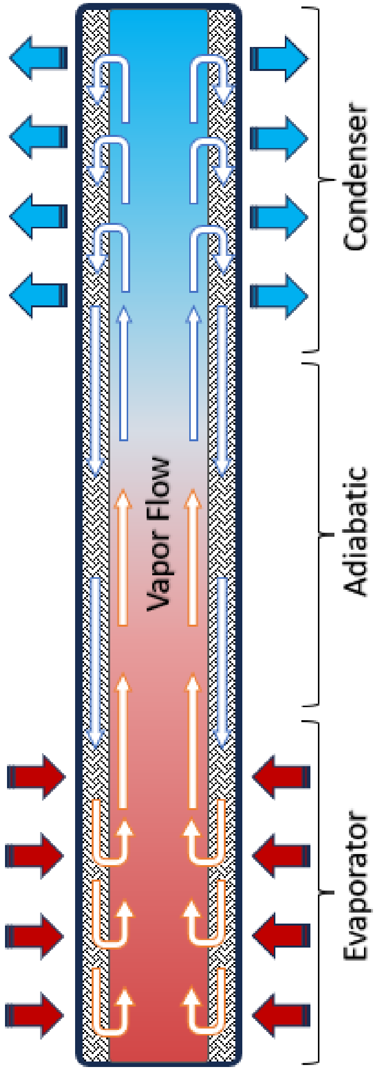

Fig 4. Vertically oriented heat pipe.

I. Introduction

➢ Motivation

- Heat pipe is an important component of heat pipe cooled micro reactors
- The performance evaluation of heat pipe should be done before licensing issues.
- Heat pipe performance is affected by factors such as working fluid, wick structure, inclination angle, aspect ratio, and filling ratio.
- Entrainment limit is a dominant heat transfer limitation in the vertical orientation.
- Existing entrainment limit correlation do not include the filling ratio effect.
- The literature about filling ratio investigation on wicked long heat pipe is rare.

➢ Objectives

- Experimental investigation of the filling ratio effect on entrainment limitation of long heat pipe.

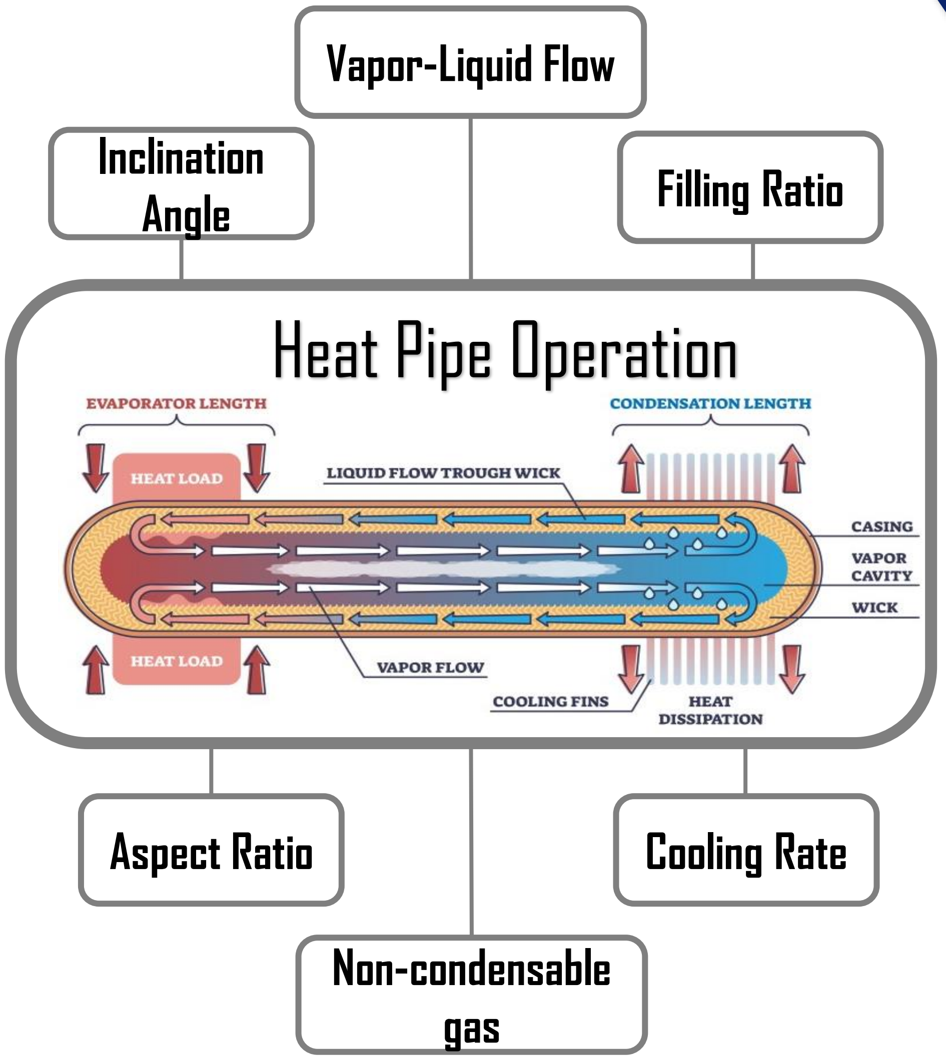

Fig. Several affecting factors.

II. Literature Survey

➢ Aspect Ratio Effects on Entrainment Limit of Thermosyphon

- Existing entrainment limit correlations do not consider the L/D effects.
- By using the *experimental results* of various L/D and pressure and *first-order fitting method*, entrainment limit was modified.

$$Q_{max} = f_4 Q_{ESDU}$$
$$f_4 = (4.788 \times 10^{-5} P_{sat} + 0.0002908)(L/D) + (-0.007704 P_{sat} + 1.273)$$

Tab. Existing entrainment limit correlations.

Researcher	Correlation
Wallis [6]	$Q_{Wallis} = C_w^2 h_{lv} A \rho_v^{1/2} [gD(\rho_l - \rho_v)]^{1/2} \left[1 + m\left(\frac{\rho_v}{\rho_l}\right)^{1/4}\right]^{-2}$
Tien and Chung [8]	$Q_{Tien\&Chung} = C_k^2 h_{lv} A \rho_v^{1/2} [g\sigma(\rho_l - \rho_v)]^{1/4} \left[1 + m\left(\frac{\rho_v}{\rho_l}\right)^{1/4}\right]^{-2}$
Katto [9]	$Q_{Katto} = \frac{0.01 \pi D_e L_e \rho_v^{0.5} h_{lv} [\sigma g(\rho_l - \rho_v)]^{0.25}}{[1 + 0.0491 L_e / D_e Bo^{0.3}]}$
Nejat [10]	$Q_{Nejat} = \frac{0.09 D_e^{1.9} L_e^{0.1} Bo^{0.5} \pi \rho_v^{0.5} h_{lv} [\sigma g(\rho_l - \rho_v)]^{0.25}}{[1 + (\rho_v/\rho_l)^{1/4}]^2}$
Imura et al. [11]	$Q_{Imura} = 0.64 \left[\frac{\rho_l}{\rho_v}\right]^{0.13} \left[\frac{D_e}{4L_e}\right] h_{lv} [\sigma g \rho_v (\rho_l - \rho_v)]^{1/4}$
ESDU [13]	$Q_{ESDU} = f_1 f_2 f_3 A h_{lv} (\rho_v)^{1/2} [g\sigma(\rho_l - \rho_v)]^{1/4}$
Faghri et al. [12]	$Q_{Faghri} = K h_{lv} A \rho_v^{1/2} [g\sigma(\rho_l - \rho_v)]^{1/4} \left[1 + m\left(\frac{\rho_v}{\rho_l}\right)^{1/4}\right]^{-2}$
Hewitt and Javanthi [14]	$Q_{Hewitt\&Javanthi} = \frac{C_w^2 h_{lv} A \rho_v^{1/2} [gD(\rho_l - \rho_v)]^{1/2}}{[1 + f(L/D)(\rho_v/\rho_l)^{1/4}]^2}$

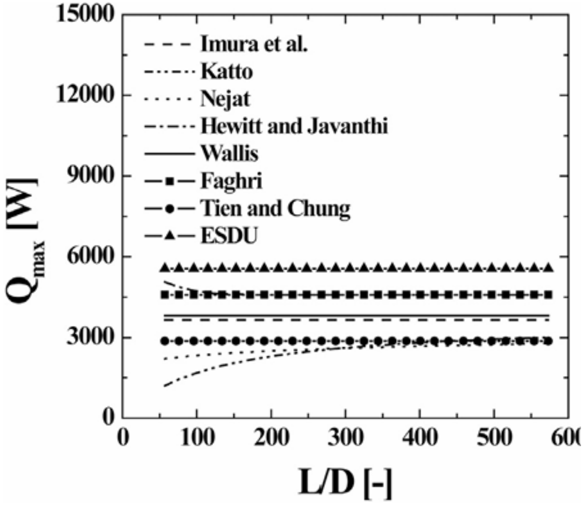

Fig. Variation in correlation prediction results for entrainment limits.

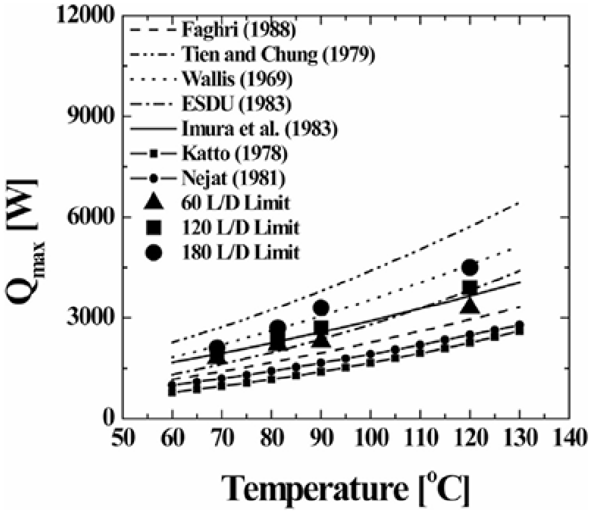

Fig. Experimental and theoretical results for entrainment limit.

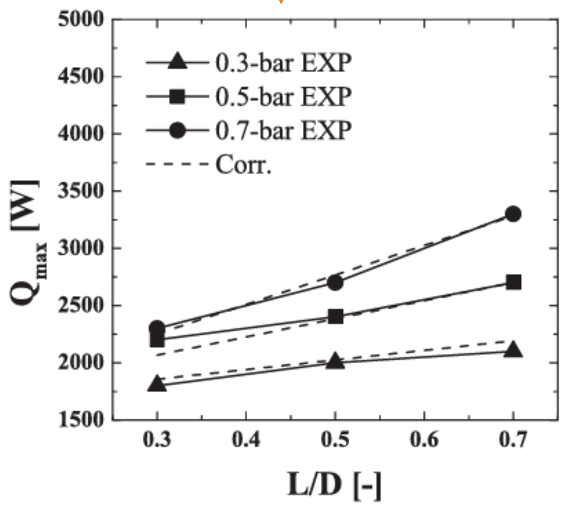

Fig. Experimental and theoretical results for entrainment limits of various heat pipes..

Tab. Experimental setup details.

Heat-pipe type	Wickless
Container	Stainless steel pipe (3/4")
Length	1, 2, 3 [m]
EAC ratio (evaporator:adiabatic region:condenser)	1:1:1
Inner diameter	16.57 [mm]
Outer diameter	19.05 [mm]
Working fluid	DI water
Heat load	600–4500 [W]
Coolant temperature	2–20 [°C]
Coolant flow rate	2–8 [lpm]
Filling ratio	100% (0.072–0.216 L)
Initial pressure (absolute pressure)	0.0013 [kPa]
Internal pressure (absolute pressure)	30, 50, 70, 200 [kPa]
Insulation	Glass fiber, aluminum foil
Measuring frequency	1 [Hz]

[1] J. Seo et al., "Length effect on entrainment limit of large L/D vertical heat pipe", International Journal of Heat and Mass Transfer, Vol. 97, pp. 751-759, 2016.
[2] J. Seo et al., "Experimental study on the startup of the annular wick type heat pipe using fiber optical temperature measurement technique", Physics of Fluids, Vol. 35, pp. 057123, 2023.

II. Literature Survey

➢ Filling Ratio Effects on Entrainment Limit of Potassium Heat Pipe

- The study aims to investigate the effects of the filling ratio and inclination angle on the thermal performance of potassium heat pipe.
- A higher filling ratio improves heat pipe performance by reducing entrainment effects.

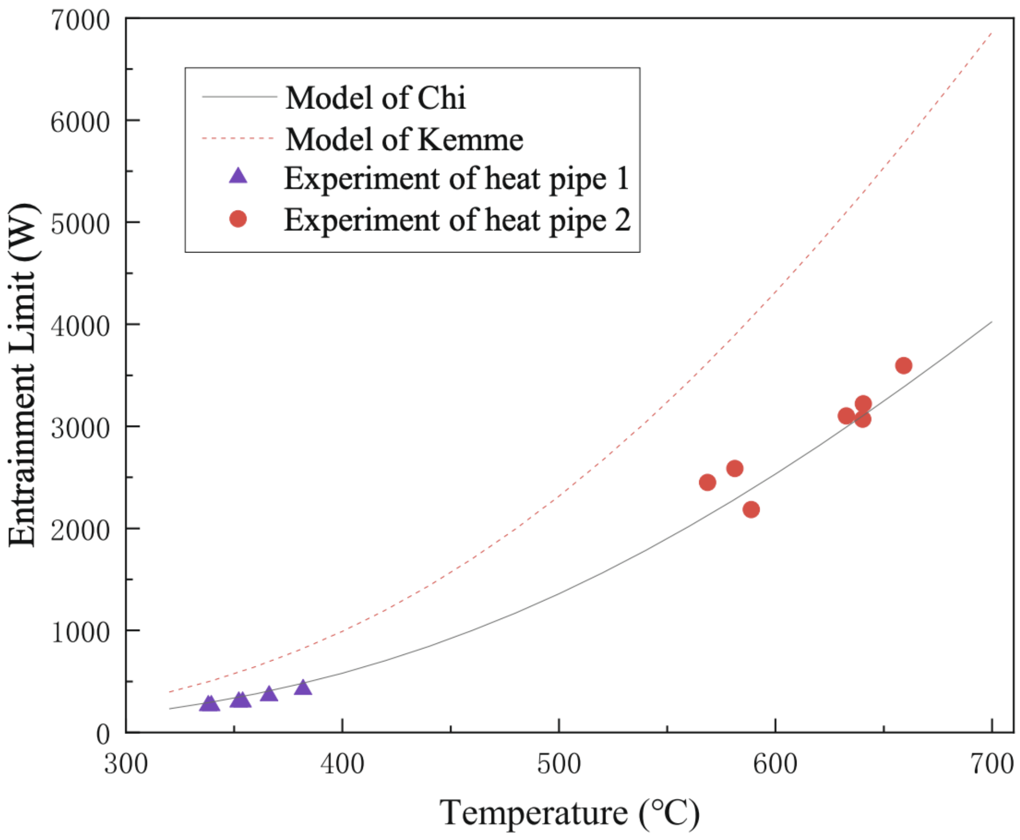

Fig. Comparison of theoretical and experimental value of entrainment limit.

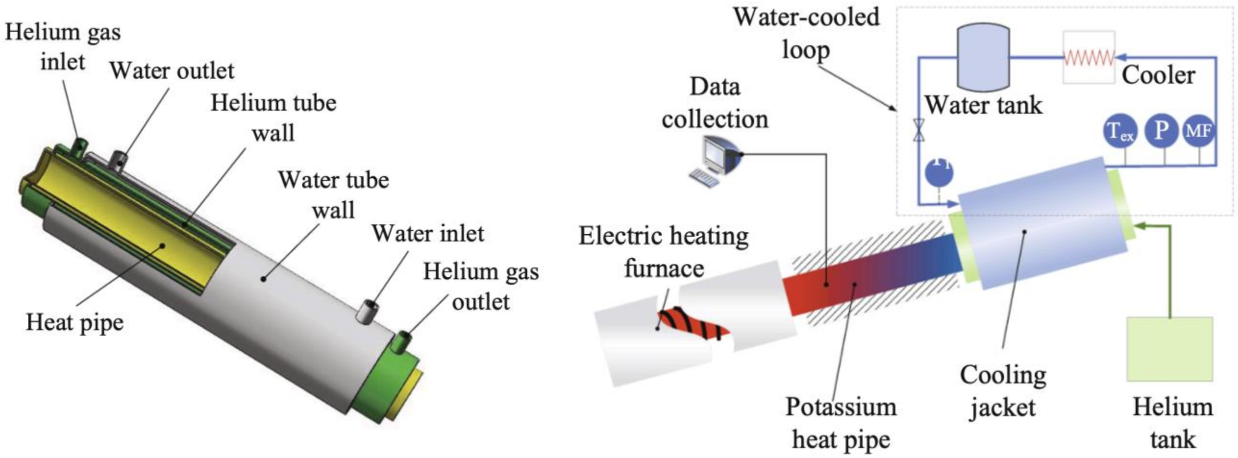

Fig 4. Schematic of the experimental system under water-cooled condition.

Tab. Experimental setup details.

Property	Value
Heat Pipe Diameter	Φ30 mm
Heat Pipe Length	800 mm
Filling Ratios	20% and 100%
Inclination Angles	0° to 90°

[3] Z. Tian, X. Liu, C. Wang, D. Zhang, W. Tian, S. Qiu, G.H. Su, "Experimental Investigation on the Heat Transfer Performance of High-Temperature Potassium Heat Pipe for Nuclear Reactor," Nuclear Engineering and Design, Vol. 378, pp. 111182, 2021.

III. Entrainment Limit and Experiment

➢ Occurrence of Entrainment Limit

- The entrainment limit is a complex issue affected by;
  - the shape of the heat pipe,
  - the behavior of the fluids.
  - the dynamics of their interaction.
- In an operating heat pipe, liquid and vapor move in opposite directions, creating a countercurrent flow.
- The countercurrent flow of liquid and vapor is influenced by shear forces at their interface, making it difficult for the liquid to return to the evaporator.
- As heat input increases;
  - the vapor velocity rises → the shear forces break the liquid's surface tension → leading to liquid droplets being carried into the vapor and towards the condenser → less liquid exist at that location → temperature increase.
- This generally happens at the and of evaporator or beginning of the adiabatic section.

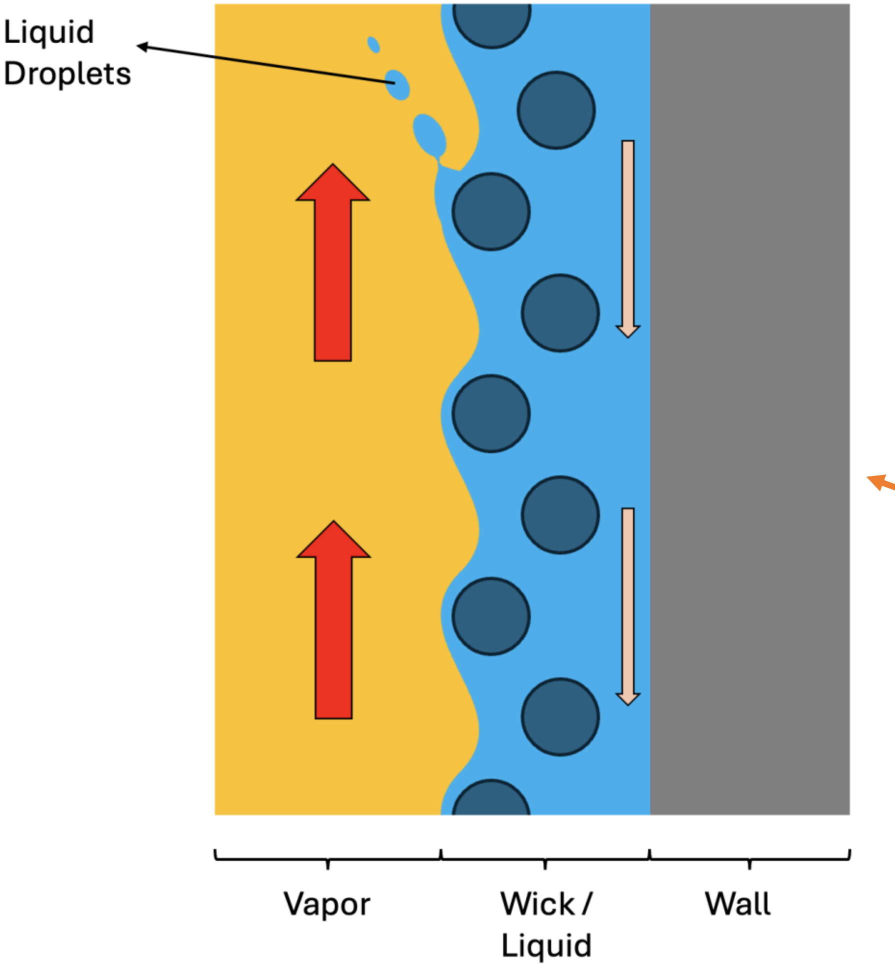

Fig. Illustration of shear-induced entrainment.

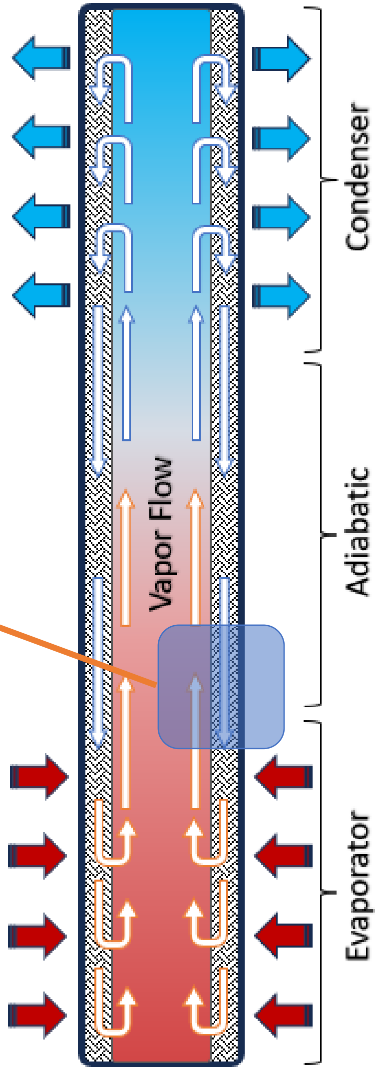

Fig 4. Vertically oriented heat pipe.

III. Entrainment Limit and Experiment

➢ Empirical Correlations

- Previous studies have proposed many models to describe the shear-induced entrainment limitation.

  - **Cotter (1976)**: Introduced hydrodynamic instability and critical wavelength for horizontally wicked heat pipes.
  - **Kemme (1976)**: Added buoyancy force to Cotter's model for gravity-assisted sodium heat pipes with screen wicks.
  - **Chi (1976)**: Developed a force balance approach for capillary-wicked heat pipes.
  - **Prenger (1984)**: Formulated a correlation for gravity-assisted heat pipes, highlighting liquid inertia over vapor inertia.
  - **Tien and Chung (1979)**: Used the Kutateladze flooding criterion for horizontal and vertical grooved heat pipes.
  - **Rice and Fulford (1987)**: Suggested that pressure difference between liquid and vapor is the kinetic head of the flow.

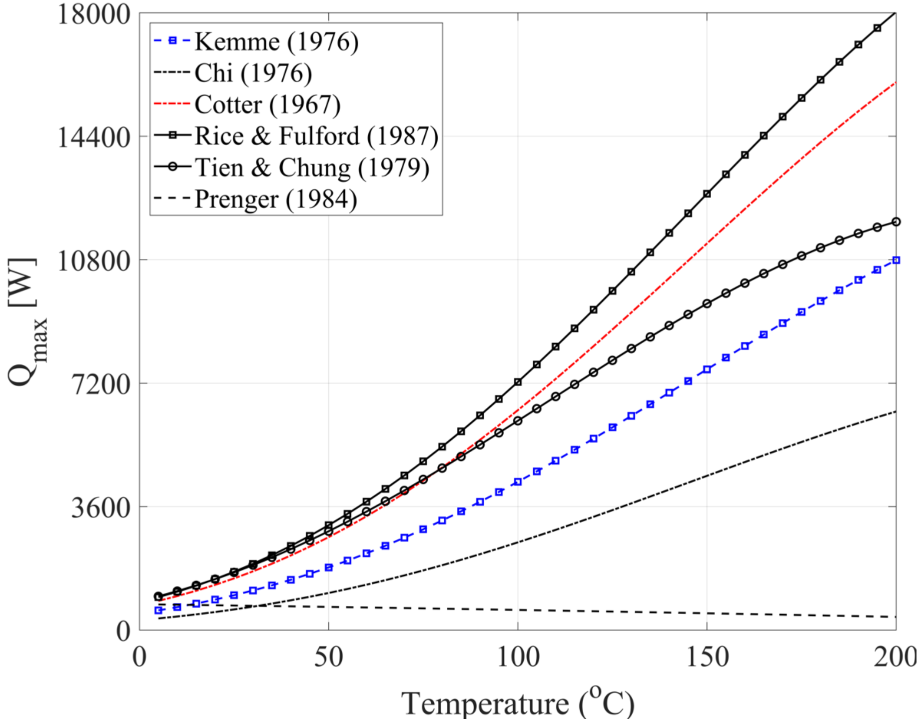

Fig. Comparison between entrainment limit correlations.

Tab. Empirical correlations for entrainment limitation of gravity-assisted he at pipe .

Researcher	Entrainment Limitation (Q_e)
Cotter (1967)	$A_v h_{fg}\left(\frac{2\pi\rho_v\sigma}{L}\right)^{1/2}$
Kemme (1976)	$A_v h_{fg}\left[\left(\frac{\rho_v}{\Omega}\right)\left(\frac{2\pi\sigma}{L}+\rho_v g D_h\right)\right]^{1/2}$
Chi (1976)	$A_v h_{fg}\left(\frac{\rho_v\sigma}{L}\right)^{1/2}$
Prenger (1984)	$2A_v h_{fg}\frac{D_{wire}}{D_{pipe}}\left(\frac{\rho_l\sigma}{\pi D_{pipe}}\right)^{1/2}$
Tien and Chung (1979)	$C_k^2 A_v h_{fg}\left(\frac{\sigma}{L}\right)^{0.5}\left(\rho_l^{-1/4}+\rho_v^{-1/4}\right)^{-2}$
Rice and Fulford (1987)	$A_v h_{fg}\left(\frac{8\rho_v\sigma}{L}\right)^{1/2}$

III. Entrainment Limit and Experiment

➢ Empirical Correlations

- The general assumption is saturated wick for entrainment limit correlations.
- According to charging amount, the wick saturation level changes.

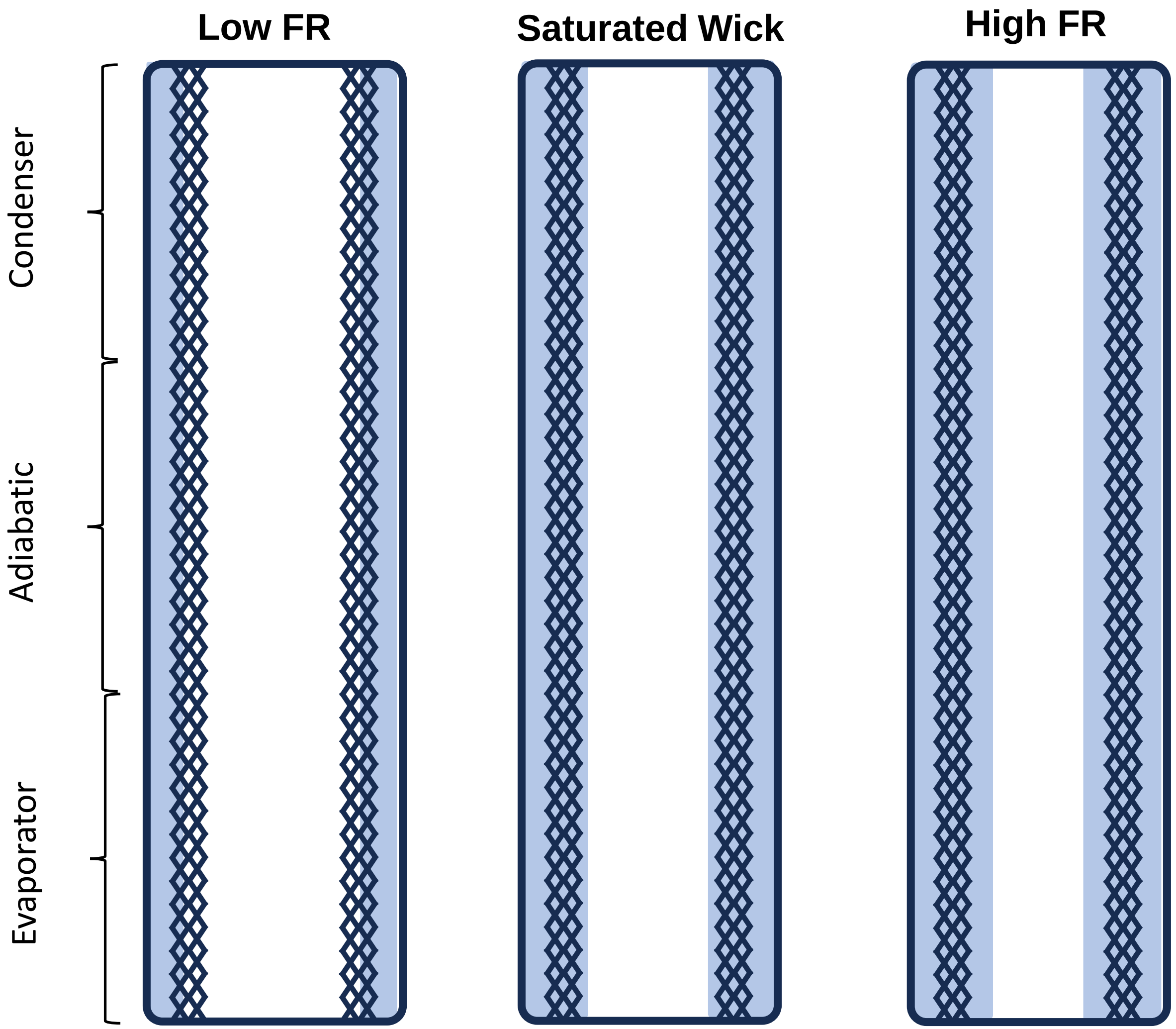

Fig. Illustration wick saturation levels.

Tab. Empirical correlations for entrainment limitation of gravity-assisted heat pipe .

Researcher	Entrainment Limitation (Q_e)
Cotter (1967)	$A_v h_{fg}\left(\frac{2\pi\rho_v\sigma}{L}\right)^{1/2}$
Kemme (1976)	$A_v h_{fg}\left[\left(\frac{\rho_v}{\Omega}\right)\left(\frac{2\pi\sigma}{L}+\rho_v g D_h\right)\right]^{1/2}$
Chi (1976)	$A_v h_{fg}\left(\frac{\rho_v\sigma}{L}\right)^{1/2}$
Prenger (1984)	$2A_v h_{fg}\frac{D_{wire}}{D_{pipe}}\left(\frac{\rho_l\sigma}{\pi D_{pipe}}\right)^{1/2}$
Tien and Chung (1979)	$C_k^2 A_v h_{fg}\left(\frac{\sigma}{L}\right)^{0.5}\left(\rho_l^{-1/4}+\rho_v^{-1/4}\right)^{-2}$
Rice and Fulford (1987)	$A_v h_{fg}\left(\frac{8\rho_v\sigma}{L}\right)^{1/2}$

III. Entrainment Limit and Experiment

➢ Experimental Setup

- 4-meter-long heat pipe with a 3D-printed combined lattice wick structure.
- Equipped with furnace heaters for consistent heating.
- Vacuum pump used to maintain the internal pressure.
- Two 4-20mA pressure transmitters located at the top and bottom of the heat pipe.
- Twenty K-type thermocouples placed at 20 cm intervals along the outer wall of the heat pipe.
- Turbine-type flow meter to measure the coolant flow rate in the cooling jacket.

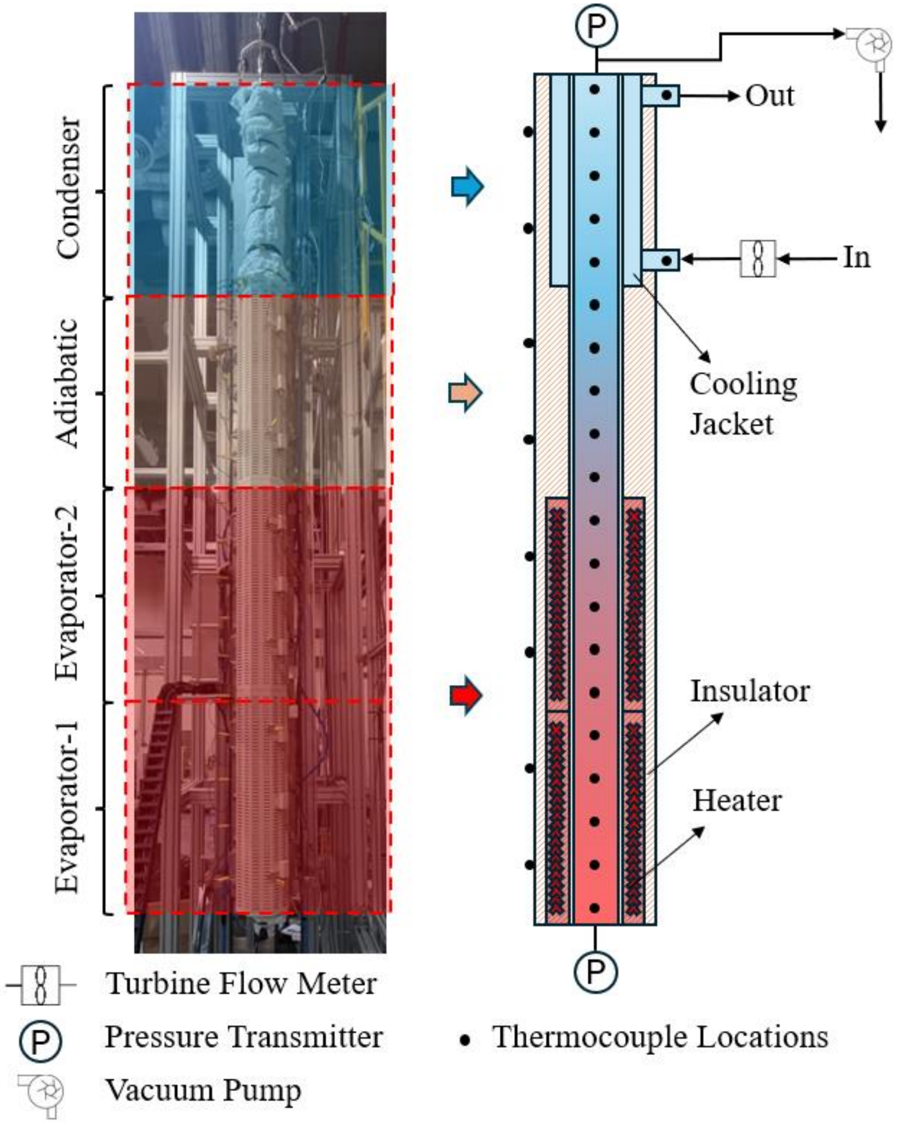

Fig. Demonstration for 4m long experimental facility.

Tab. Experimental system parameters.

Parameter	Value
Working Fluid	DI Water
Length of Eva/Adia/Cond (m)	2 / 1 / 1
Pipe Inner Diameter (mm)	22.0
Pipe Outer Diameter (mm)	25.4
Wick Type	Combined Wick
Wick Inner Diameter (mm)	14.0
Wick Outer Diameter (mm)	20.0
Porosity	0.44
Initial Pressure (kPa)	101, 75, 50
Filling Ratio	120%, 100%, 80%, 60%
Inclination	Vertical
HX Coolant	Tap Water
Flow Rate (lpm)	0.05 ~ 2.5
Power Input (kW)	0~8
Orientation	Vertical

IV. Results

➢ Variable filling ratio with constant pressure

- The detection of the entrainment limitation in a heat pipe is achieved primarily by monitoring temperature fluctuations within the system.

80% FR, 101 kPa

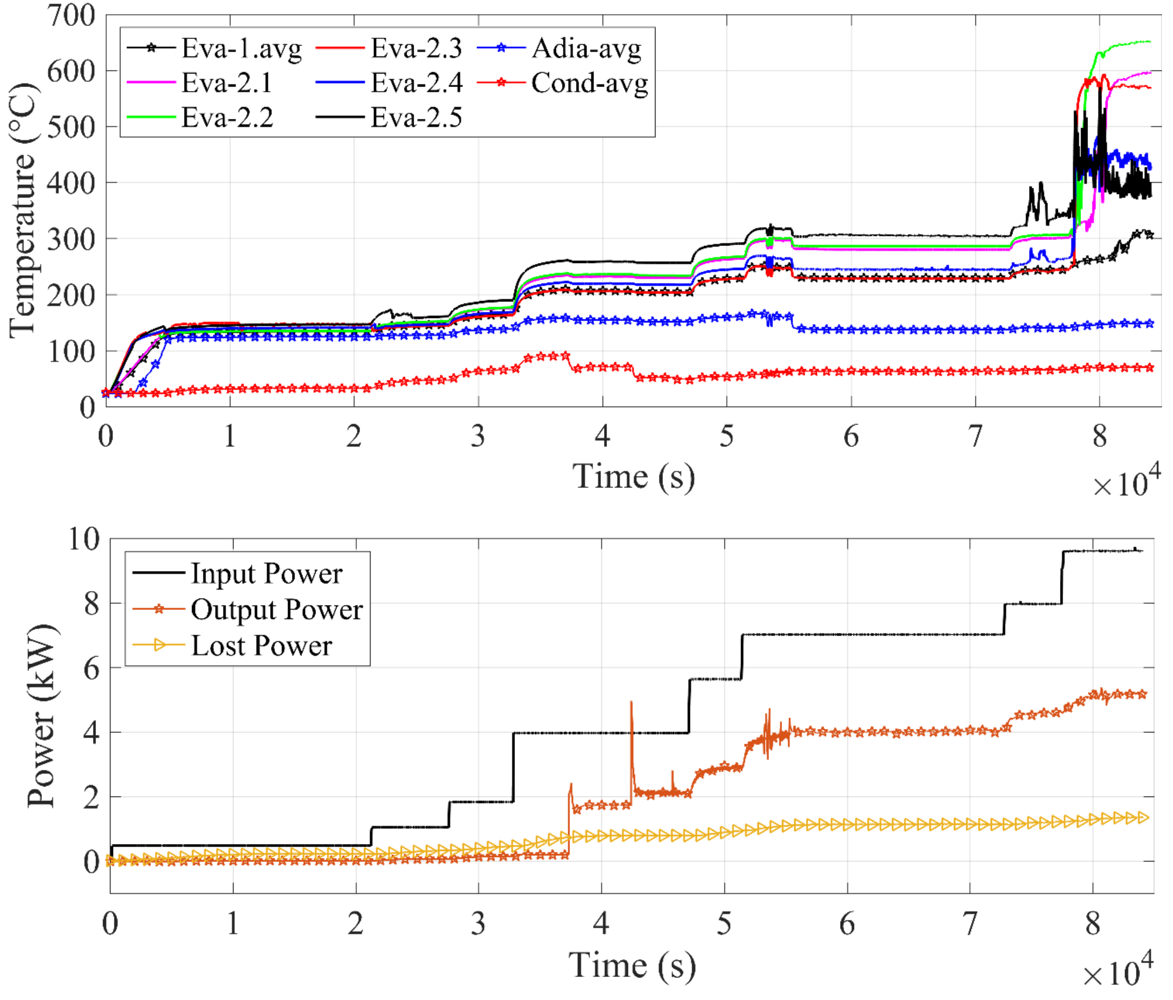

120% FR, 101 kPa

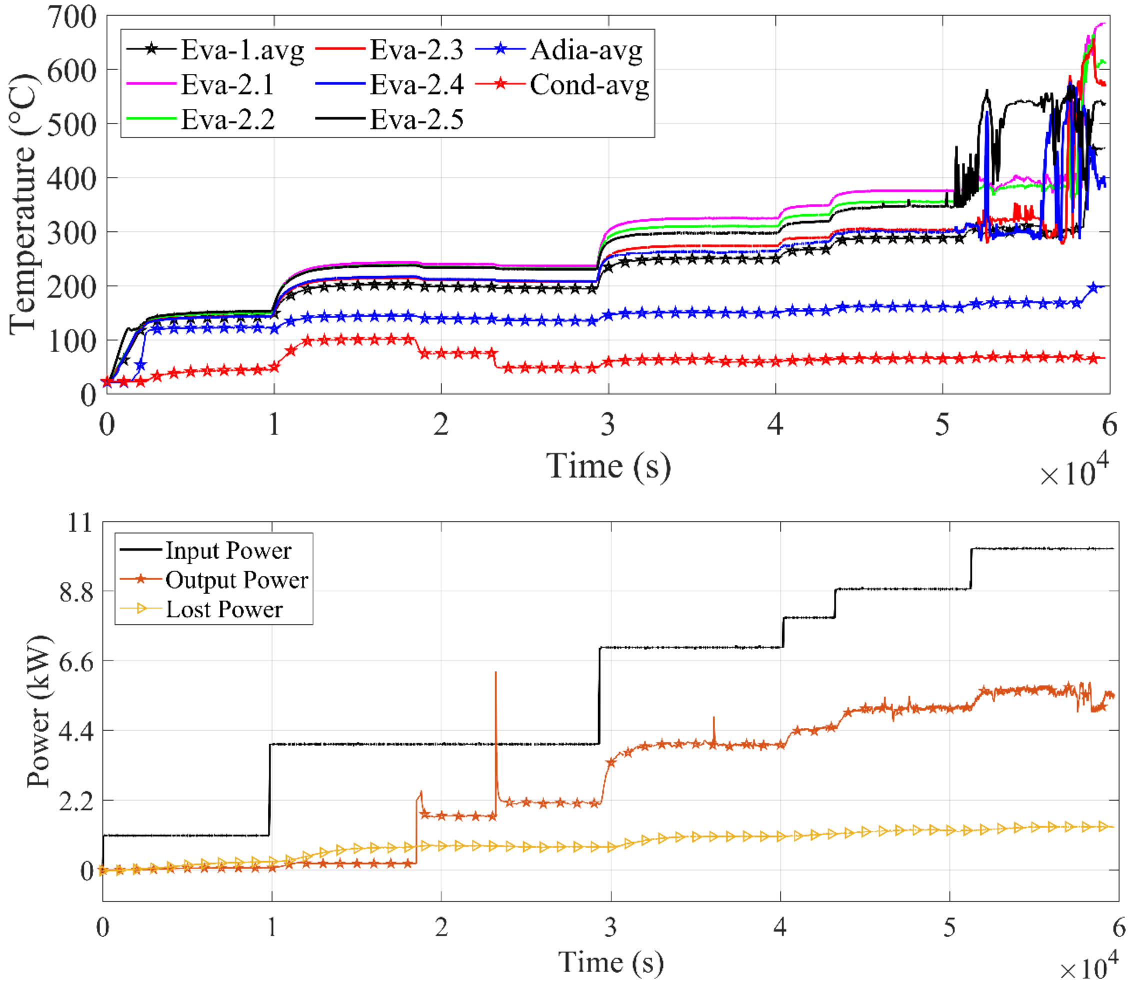

IV. Results

➢ Variable pressure with constant filling ratio

- The detection of the entrainment limitation in a heat pipe is achieved primarily by monitoring temperature fluctuations within the system.

100% FR, 101 kPa

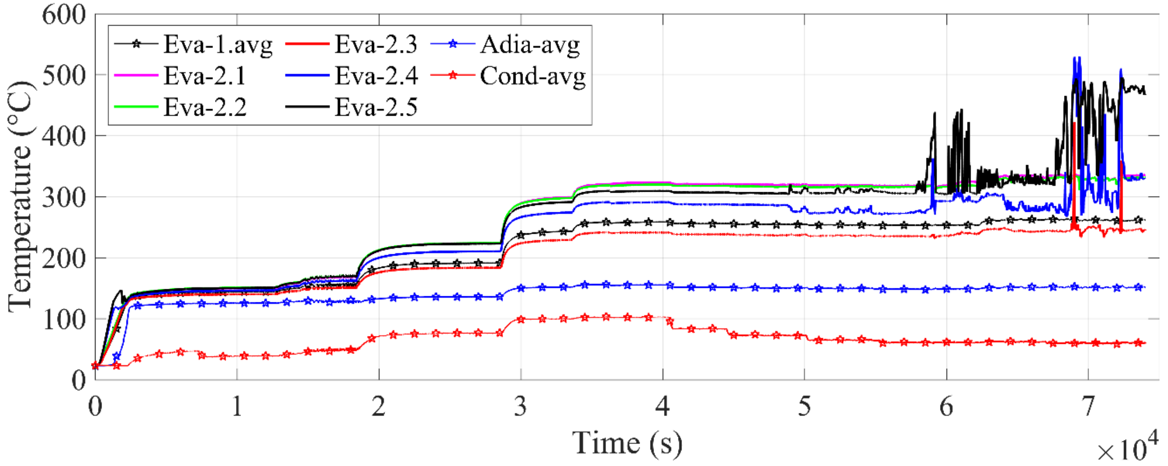

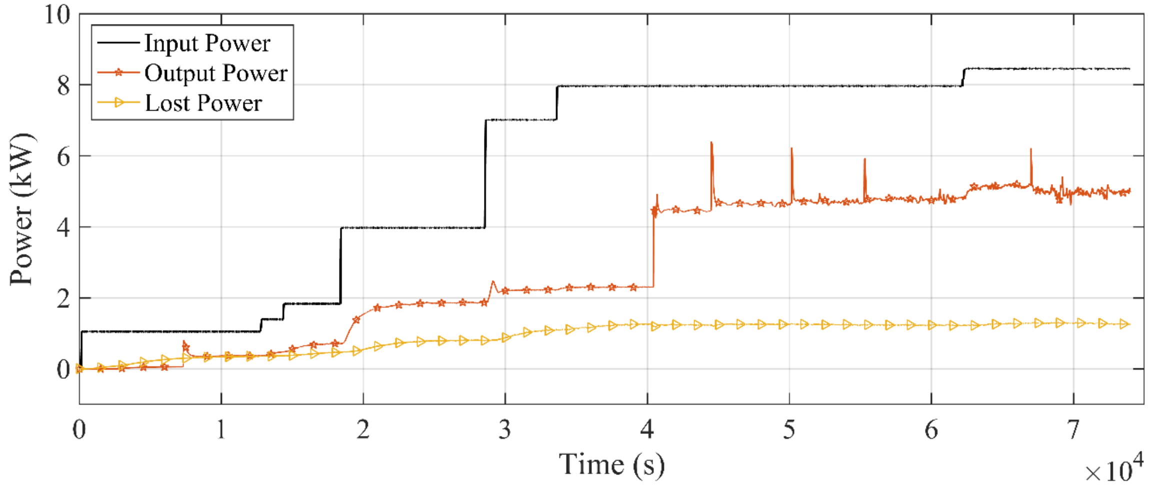

100% FR, 50 kPa

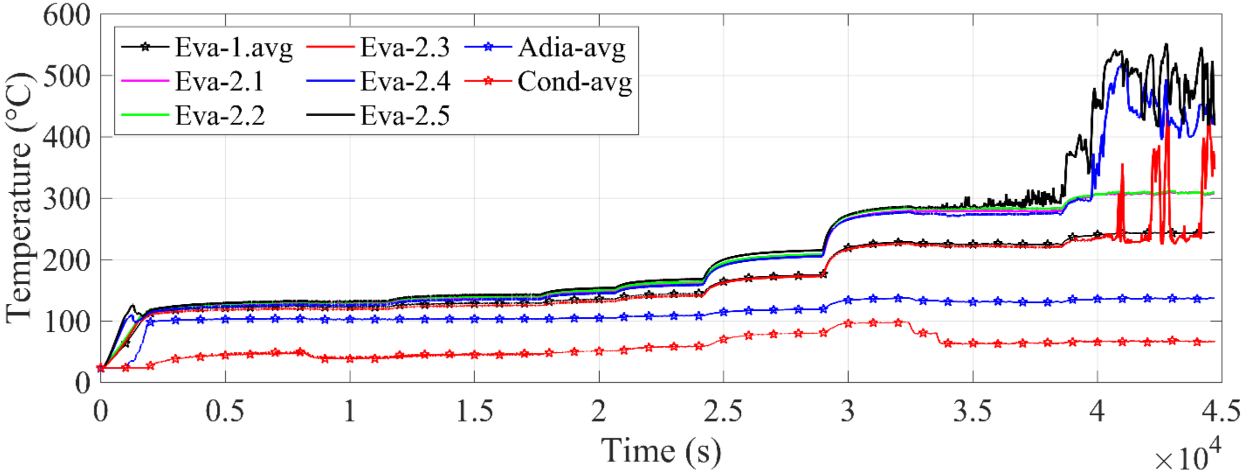

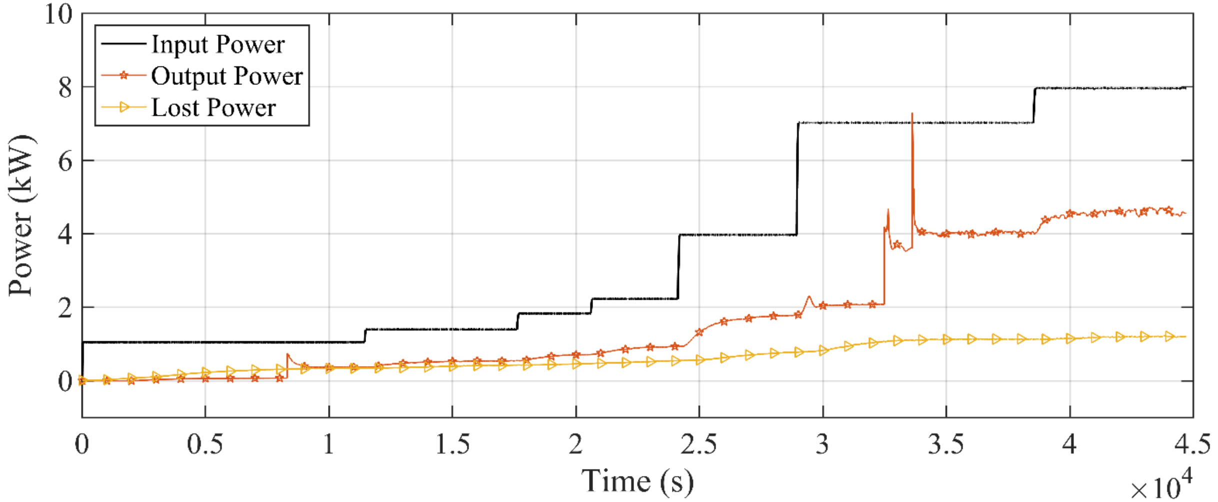

IV. Results

➢ Comparison with Correlations

- Most theoretical models overestimate maximum heat transfer capacity compared to experimental results, especially at lower filling ratios.
- Chi's model matches experimental data well for 120%, 100% and 80% filling ratios, making it more suitable for systems with higher fluid content.
- Prenger's model is more accurate for 60% filling ratio, suggesting its suitability for systems with lower wick saturation levels.

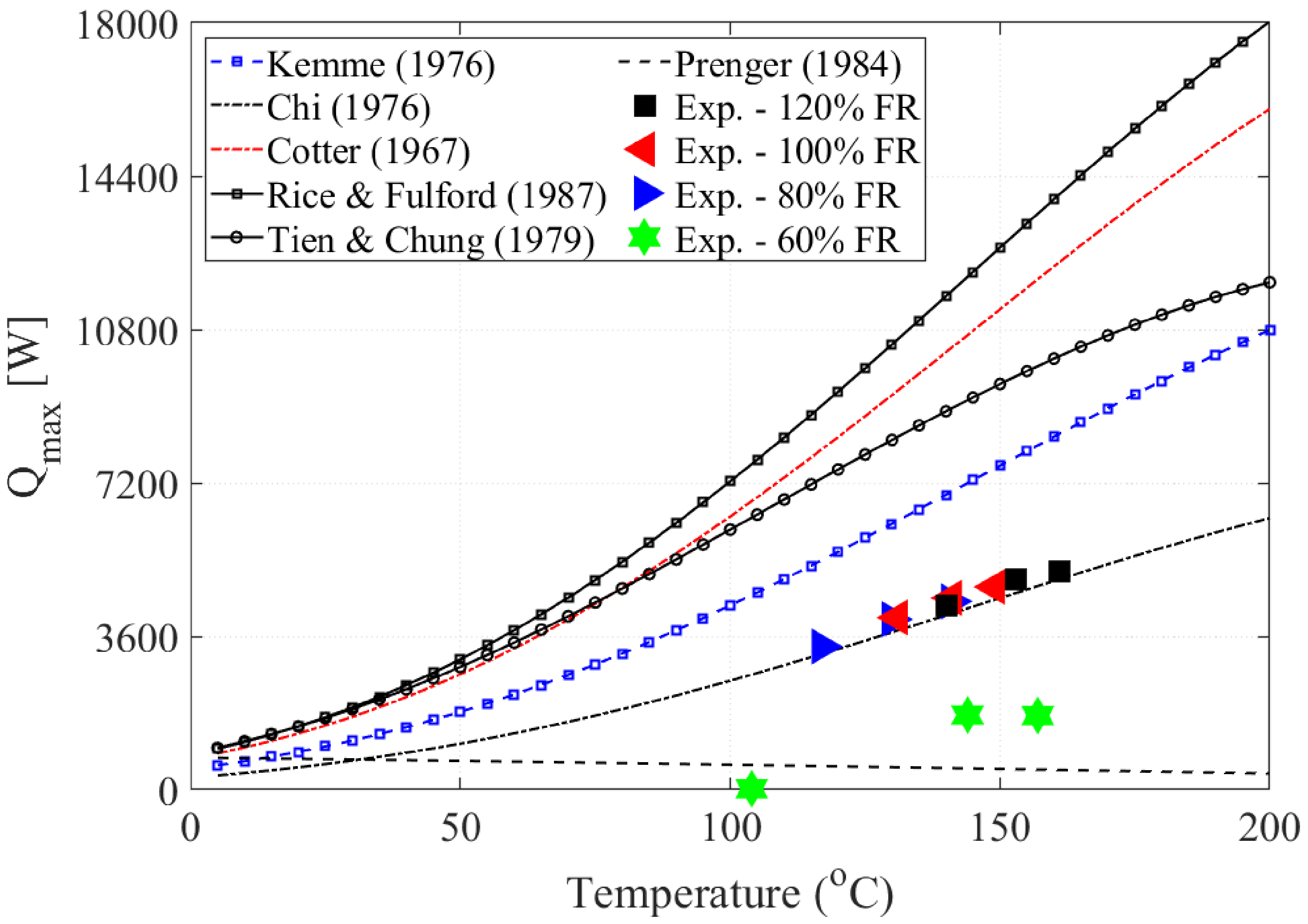

Fig. Comparison between entrainment limit correlation and experimental results.

IV. Results

➢ Comparison for Steady-State operation

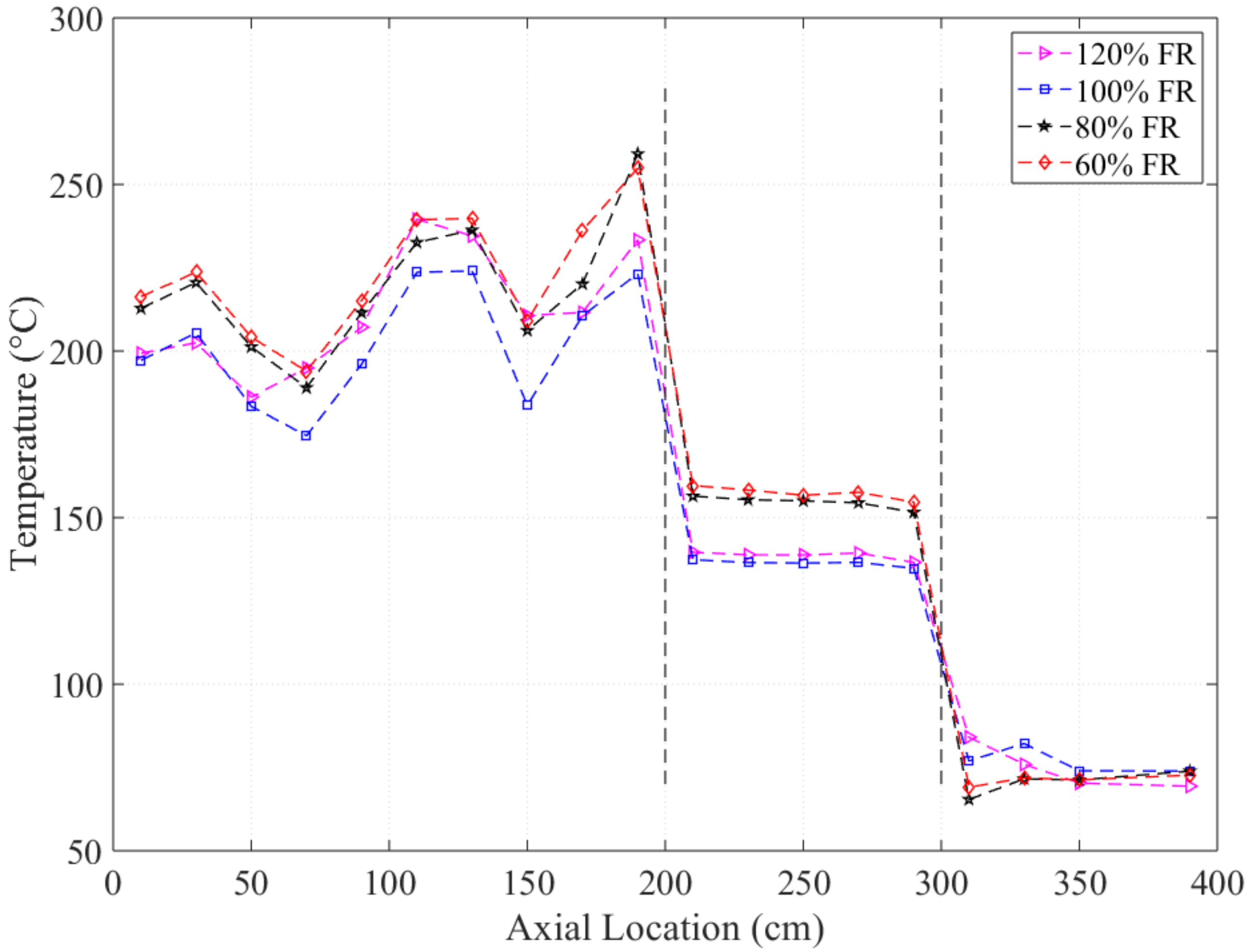

Fig. Steady-state temperature profiles at 3970 W and 0.55 lpm coolant flow rate.

- Despite different filling ratios, the temperature profiles show similar overall trends.
- The 60% filling ratio has the highest temperature profile, especially in the evaporator section of the heat pipe.
- The higher temperature in the 60% filling ratio indicates less effective cooling due to reduced liquid content, leading to higher operating temperatures.

V. Conclusion and Future Works

➢ Conclusion

- The study investigated the effect of filling ratio on the entrainment limit of a large-scale heat pipe with a 3D-printed wick structure.
- Filling ratio significantly affects the heat pipe's thermal performance and stability, particularly concerning the onset of entrainment.
- Higher filling ratios result in better thermal management and delay the onset of entrainment.
- Lower filling ratios cause increased temperature fluctuations and earlier instability.
- Comparison with theoretical models shows Chi's model predicts well for higher filling ratios, while Prenger's model is more accurate for lower filling ratios.
- The study emphasizes the need for refinement of theoretical models to better capture varying operational conditions.

➢ Future Works

- Additional experimental investigation of several filling ratio to understand well the entrainment occurrence.
- Similar investigations will be conducted for different inclination angles.
- The entrainment limit correlation will be modified according to experimental results.

Thanks for your attention.

UNIST Reactor Innovation Loop (URI-LO)